

The 1/1 and 2/1 Approximants in the Sc–Mg–Zn Quasicrystal System: Triacotahedral Clusters as Fundamental Building Blocks

Qisheng Lin and John D. Corbett*

Contribution from the Department of Chemistry, Iowa State University, Ames, Iowa 50011

Received June 3, 2006; E-mail: jcorbett@iastate.edu

Abstract: Single-crystal structures are reported for $\text{Sc}_3\text{Mg}_{0.18(1)}\text{Zn}_{17.73(3)}$, the 1/1 approximant crystal (AC), and $\text{Sc}_{11.18(9)}\text{Mg}_{2.5(1)}\text{Zn}_{73.6(2)}$, the 2/1 AC, in the corresponding icosahedral quasicrystal (i-QC) system. The 1/1 AC crystallizes in space group $Im\bar{3}$, $a = 13.863(2)$ Å, $Z = 8$, and the 2/1 AC, in $Pa\bar{3}$, $a = 22.412$ (2) Å, $Z = 8$. The latter, which is valuable in pointing the way to the QC structure, is the best ordered and refined 2/1 example to date. The fundamental building blocks in both ACs are triacotahedral clusters centered by smaller multiply endohedral Tsai-type arrays; the former are condensed through body-centered-cubic packing in the 1/1 and primitive cubic packing in the 2/1 AC. Novel prolate rhombohedra centered by Sc–Sc dimers are also generated between triacotahedra in the 2/1 AC.

Introduction

Icosahedral quasicrystals (i-QCs) are novel intermetallic compounds that exhibit $m\bar{3}5$ symmetry,^{1–3} which puts them beyond the capabilities of classical crystallography because of the forbidden 5-fold rotational symmetry. However, neighboring crystalline compounds—approximant crystals (ACs)—have nearby chemical compositions and presumably similar local building blocks to those in the corresponding QC.⁴ The cell parameters ($a_{q/p}$) of successive ACs are related to the QC lattice constant (a_6) by $a_{q/p} = 2a_6(p + q\tau)/\sqrt{(2 + \tau)}$,⁴ in which $\tau = 1.618$, the golden mean, and p and q , are two consecutive Fibonacci numbers. Accordingly, an i-QC can be considered as a cubic AC with an infinite lattice constant, and the higher the order (q/p) of an AC, the closer its structure approaches that of the i-QC. Hence, the structures of higher order ACs play important roles in structural modeling of corresponding i-QC.

Recently, the discovery of the first binary i-QCs as $\text{MCD}_{5.67}$ ($\text{M}=\text{Ca}, \text{Yb}$) by Tsai et al.⁵ aroused extensive interest. According to the structures of the corresponding MCD_6 1/1 ACs^{6,7} (space group $Im\bar{3}$), the binary i-QCs have been assumed to contain the same 66-atom four-shell $\text{M}_{12}\text{Cd}_{54}$ complex clusters as building blocks.⁵ Similar structural motifs have since been named Tsai-type clusters.^{8,9} These contain, from the center out,

a 3-fold disordered Cd_4 tetrahedron, a Cd_{20} pentagonal dodecahedron, a M_{12} icosahedron, and a Cd_{30} icosidodecahedron. Of course, the disordered tetrahedron is internally symmetry-breaking, stimulating questions as to how these are altered or assembled in the i-QC. These clusters are noteworthy in that they exhibit a new short-range-order (SRO), different from the well-known Bergman¹⁰ and Mackay types¹¹ in other systems that exhibit 104-atom four-shell and 54-atom three-shell multiply endohedral arrangements, respectively.

Numerous ternary or quaternary Tsai-type i-QCs are now known in the Sc–M–Zn ($\text{M} = \text{Mg}, \text{Mn}, \text{Fe}, \text{Co}, \text{Ni}, \text{Cu}, \text{Pd}, \text{Pt}, \text{Au}, \text{Ag}$),^{8,9,12} the Sc–Mg–Cu–Ga,^{13,14} and the A–M–In ($\text{A} = \text{Ca}, \text{Yb}; \text{M} = \text{Au}, \text{Ag}$) systems.¹⁵ Of these, the Sc–Mg–Zn i-QC has been stated to be the best of the Tsai-type i-QCs examined in terms of structural perfection.^{8,9} But the structures of most ternary 1/1 ACs are still not known except for $\text{Sc}_3\text{Cu}_y\text{Zn}_{18-y}$ ($0 \leq y \leq 2.2$)¹⁶ and $\text{Sc}_3\text{Mg}_{0.17}\text{Cu}_{10.5}\text{Ga}_{7.34}$.¹³ So far, $\text{M}_{13}\text{Cd}_{76}$ ($\text{M} = \text{Ca}, \text{Yb}$)^{17,18} are the only reported Tsai-type 2/1 ACs that have been structurally refined from single-crystal X-ray diffraction data. The binary nature of these two 2/1 ACs perhaps offers the best possibilities to avoid the occupation disorder that usually occurs in multicomponent intermetallic compounds. However, both structures are still imperfect and

- (1) Janot, C. *Quasicrystals: A Primer*, 2nd ed.; Oxford University Press: Oxford, U.K., 1994.
- (2) Shechtman, D.; Blech, I.; Gratias, D.; Cahn, J. W. *Phys. Rev. Lett.* **1984**, *53*, 1951.
- (3) Hahn, T.; Klapper, H. In *Intl. Tab. Crystallogr.*, 5th ed.; Hahn, T., Ed.; Kluwer Academic Publisher: Dordrecht/Boston/London, 2002; Vol. A, pp 761–803.
- (4) Goldman, A. I.; Kelton, K. F. *Rev. Mod. Phys.* **1993**, *65*, 213.
- (5) Tsai, A. P.; Guo, J. Q.; Abe, E.; Takakura, H.; Sato, T. *J. Nature* **2000**, *408*, 537.
- (6) Villars, P.; Calvert, L. D. *Pearson's Handbook of Crystallographic Data for Intermetallic Phases*, 2nd ed.; American Society of Metals: Materials Park, OH, 1991; Vol. 1.
- (7) Pay Gómez, C.; Lidin, S. *Phys. Rev. B: Condens. Matter Mater. Phys.* **2003**, *68*, 024203.

- (8) Ishimasa, T.; Kaneko, Y.; Kaneko, H. *J. Non-Cryst. Solids* **2004**, *334–335*, 1.
- (9) Ishimasa, T. In *The Science of Complex Alloy Phases*; Massalski, T. T.; Turchi, P. E. A., Eds.; TMS (The Mineral, Metals & Materials Society): Warrendale, PA, 2005; pp 231–249.
- (10) Bergman, G.; Waugh, J. L. T.; Pauling, L. *Acta Cryst.* **1957**, *10*, 254.
- (11) Mackay, A. L. *Acta Crystallogr.* **1952**, *15*, 916.
- (12) Lin, Q.; Corbett, J. D. *Philos. Mag.* **2006**, *86*, 607.
- (13) Lin, Q.; Corbett, J. D. *J. Am. Chem. Soc.* **2005**, *127*, 12786.
- (14) Kaneko, Y.; Maezawa, R.; Kaneko, H.; Ishimasa, T. *Phil. Mag. Lett.* **2002**, *82*, 483.
- (15) Lin, Q.; Corbett, J. D. To be submitted for publication.
- (16) Lin, Q.; Corbett, J. D. *Philos. Mag. Lett.* **2003**, *83*, 755.
- (17) Pay Gómez, C.; Lidin, S. *Angew. Chem., Int. Ed.* **2001**, *40*, 4037.
- (18) Pay Gómez, C. *Order and Disorder in the RE–Cd and related systems*; Stockholm University, Sweden, 2003.

show several configuration disorders.^{17,18} Therefore, syntheses and structural analyses of more ACs of novel Tsai-type QC systems are highly desired.

We have recently obtained both the 1/1 and 2/1 ACs as well as the i-QC in the Sc–Mg–Zn system¹² by means of synthetic explorations aided by electronic/composition tuning directed by pseudogap predictions.¹³ In this paper, the detailed structures of the two ACs will be presented, from which triacontahedral clusters, rather than smaller Tsai-type clusters within them, are clearly established as the basic building blocks in both. These give an important basis for the construction of an iceberg model of i-QC.¹⁵

Experimental Section

Syntheses. Crystals of $\text{Sc}_3\text{Mg}_{0.18(1)}\text{Zn}_{17.73(3)}$, the 1/1 AC, and of $\text{Sc}_{11.18(9)}\text{Mg}_{2.5(1)}\text{Zn}_{73.6(2)}$, the 2/1 AC according to structural analyses, were first obtained from reactions of $\text{Mg}_{2-x}\text{Sc}_x\text{Zn}_{11}$ compositions with $x = 1.82$ and 0.75 , respectively.¹² As-received Sc chunks (99.9%, APL–Aldrich), Mg turnings, and Zn granules (both 99.9%, Alfa) were weighed in a glovebox under a nitrogen atmosphere and weld-sealed into tantalum containers under Ar, as before.¹⁹ These were in turn held within evacuated and sealed SiO_2 jackets to avoid air oxidation. Samples were first heated to 700 °C, held at this temperature for 3 days, slowly cooled (5 °C/hr) to 400 °C for crystal growth, and then annealed at this temperature for 2 days. Both phases, which were obtained in high yield (>90%), are air stable at room temperature. More details about the syntheses, the tuning process, the phase widths of the two ACs, the 1/1 atom coordinates, and the electronic structure calculations on the 1/1 AC have been presented in a conference paper.¹²

Powder X-ray Diffraction. Phase analyses were carried out by powder X-ray diffraction. Data acquisition was performed on a Huber 670 Guinier powder camera equipped with an area detector and Cu $K\alpha_1$ radiation ($\lambda = 1.540598$ Å). Powders were homogeneously dispersed on a flat mylar film with the aid of petrolatum grease. The step length was set at 0.005°, and the exposure time was 0.5 h.

SEM-EDX Analyses. The elemental compositions were determined via semiquantitative energy-dispersive X-ray spectroscopy (EDX) with the aid of a JEOL 840A scanning electron microscope (SEM) with an IXRF X-ray analyzer system and Kevex Quantum light-element detector. A beam of 20 kV and 0.3 mA was used to gain count rates of about 2500 s⁻¹. To increase the accuracies, the samples were mounted in epoxy and carefully polished so as to avoid the influence of sample tilting. During measurements, samples were first scanned by back-scattered-electron techniques, from which phases with different compositions were clearly revealed by their different darkensses. Then the detector was focused on each phase region to acquire at least four readings of the spectrum. Averaged values were used in comparison with the refined compositions from X-ray structural analyses.

X-Ray Single-Crystal Diffraction. Data collections for $\text{Sc}_3\text{Mg}_{0.18(1)}\text{Zn}_{17.73(3)}$, the 1/1 AC, and $\text{Sc}_{11.18(9)}\text{Mg}_{2.5(1)}\text{Zn}_{73.6(2)}$, the 2/1 AC, were performed at room temperature with the aid of a Bruker APEX Platform CCD diffractometer equipped with graphite-monochromatized Mo $K\alpha$ radiation. The data sets were each collected over one hemisphere with an acquisition time of 10 s per frame. Data integration and absorption and Lorentz polarization corrections were done by the SAINT and SADABS subprograms in the SMART software packages.²⁰ Cell parameters were refined from reflections with $I/\sigma(I) > 20$. Structure determinations and refinements were performed with the SHELXTL subprogram. The assignment of the space group was made on the basis of the Laue symmetries determined by the diffractometer programs and systematic absence analyses.

The 1/1 AC was found to crystallize in a cubic space group $Im\bar{3}$ (No. 204), with $a = 13.863(2)$ Å. Direct methods were used to establish an initial structural model of seven atoms. Environmental analyses revealed six of them had separations (2.51–2.84 Å) suitable for Zn–Zn bonds and the other (2.92–3.04 Å) for Sc–Zn separations, and these were so assigned initially. After a few cycles of refinement, the $R1$ value converged at ~12.6%. Examination of the isotropic displacement parameters revealed that Zn3 and Zn7 had somewhat larger isotropic values ($U_{\text{eq}} = 0.023$ and 0.027 Å², respectively) than the average for the others (0.011 Å²), suggesting possible mixing with Mg. Such mixtures were allowed for each position during isotropic refinements with the total occupancy of each constrained to unity. Results showed that all positions were free of Mg within 2σ standard deviations except that Zn7/Mg had a proportion of 0.89/0.11(3). At this stage, a Fourier map afforded another lower density position that had short distances to both a neighbor at ~2.26 Å and to itself at ~1.56 Å. It was recognized that partial occupancy (~33%) by an atom in this position would define a disordered tetrahedron, as had been typically refined in several MgCd_6 and in ScZn_6 .²¹ Thus, the site was assigned to Zn4, and its occupancy constraint was removed in subsequent isotropic refinements, during which the $R1$ value decreased to ~11.0%. Finally, least-square refinements with anisotropic parameters converged at $R1 = 2.64\%$, $wR2 = 5.50\%$, $\text{GOF} = 1.113$ for 47 parameters and 613 independent reflections ($I > 2\sigma(I)$).

The refined composition was $\text{Sc}_3\text{Mg}_{0.18(1)}\text{Zn}_{17.73(3)}$, or normalized as $\text{Sc}_{14.35}\text{Mg}_{0.86(5)}\text{Zn}_{84.79(14)}$, in excellent agreement with the EDX data, $\text{Sc}_{14.8(1)}\text{Mg}_{0.8(1)}\text{Zn}_{84.4(5)}$. A small Mg content is also essential to the formation of the Sc–Mg–Zn i-QC, which has the nearby composition $\text{Sc}_{14.6(4)}\text{Mg}_{3.3(4)}\text{Zn}_{82.1(2)}$.¹² The very anisotropic character of Zn4 in the tetrahedron is structurally inherent, and no better model than a 3-fold disordered tetrahedron can evidently be used to better represent the observed electron density (figure S1), as in the prototype YCd_6 .²² Pay Gómez and Lidin have found similar but also more complex cases in studies of diverse MgCd_6 structures.⁷ Because of the disorder, atoms in this shell always have the largest displacements ($U_{\text{eq}} > 0.03$ Å²), and those in the next dodecahedral shell have correspondingly slightly increased displacement parameters ($U_{\text{eq}} \approx 0.02\text{--}0.03$ Å²). On the contrary, atoms in the other shells usually have normal displacement parameters ($U_{\text{eq}} < 0.02$ Å²), and the same is true for the 2/1 AC (below).

The 2/1 AC was found to crystallize in space group $Pa\bar{3}$ (No. 205), with $a = 22.412(2)$ Å. Similarly, direct methods first afforded 32 atomic positions, and environmental analyses revealed two groups of distances, 26 positions with separations suitable for Zn–Zn bonds and five others at greater distances suitable for Sc–Zn pairs, and these were so assigned. After a few cycles of isotropic refinement, $R1$ converged at ~13.0%. Analyses of the difference Fourier map suggested another weakly diffracting position, and examination of its environment revealed that an atom at this position would have reasonable bond distances to Zn19 and Zn23 at about 2.84 and 2.99 Å, respectively, plus a very short distance (1.27 Å) to Zn26. Thus, the weak peak was assigned as Zn27, and the occupancies of Zn26 and Zn27 were refined in subsequent steps to 44(2) and 28(2)%, respectively. Subsequent isotropic refinements also yielded somewhat larger isotropic displacement parameters for Sc2, Zn16, and Zn23 compared with the average of the others (0.012 Å² excluding Zn27). This suggested that Sc2 and Zn16 were mixed with Mg, whereas the Zn23 site was refined partially occupied (87-(1)%) because it forms a fractional tetrahedron with Zn27. They were so assigned (with total occupancies constrained to 100% for mixed positions) in the following isotropic refinements, which converged at $R1 = 11.3\%$ with well-defined Zn/Mg and Sc/Mg proportions on only two sites. The final anisotropic refinements resulted in $R1 = 6.63\%$, $wR2 = 12.01\%$, and $\text{GOF} = 1.016$ for 273 parameters and 4617

(19) Lin, Q.; Corbett, J. D. *Inorg. Chem.* **2003**, *42*, 8762.

(20) SHELXTL; Bruker, AXS Inc.: Madison, WI, 1997.

(21) Lin, Q.; Corbett, J. D. *Inorg. Chem.* **2004**, *43*, 1912.

(22) Larson, A. C.; Cromer, D. T. *Acta Cryst.* **1971**, *27B*, 1875.

Table 1. Crystal Data and Structure Refinements for $\text{Sc}_3\text{Mg}_{0.18(1)}\text{Zn}_{17.73(3)}$ and $\text{Sc}_{11.18(9)}\text{Mg}_{2.5(1)}\text{Zn}_{73.6(2)}$

formula	$\text{Sc}_3\text{Mg}_{0.18(1)}\text{Zn}_{17.73(3)}$	$\text{Sc}_{11.18(9)}\text{Mg}_{2.5(1)}\text{Zn}_{73.6(2)}$
formula weight	1298.08	5383.22
space group, Z	$Im\bar{3}$, 8	$Pa\bar{3}$, 8
lattice parameter, a (Å)	13.863(2)	22.412(2)
vol.(Å ³)/ d_{cal} (g/cm ³)	2664.2(5)/6.473	11257.5(2)/6.344
abs. coeff. (mm ⁻¹) (Mo K α)	32.606	31.924
refl. coll./indep. obs./ R_{int}	8391/613/0.0475	68875/4617/0.1498
data/restra./param.	613/0/47	4617/0/273
GOF	1.113	1.016
$R1/wR2$ [$I > 2\sigma(I)$]	0.0264/0.0550	0.0663/0.1201
$R1/wR2$ (all data)	0.0320/0.0564	0.1326/0.1440
residue peak/hole (e.Å ⁻³)	3.30/−1.63	4.98/−2.63

independent reflections ($I > 2\sigma(I)$). The maximal and minimal residue peaks were 4.98 (~ 1.1 Å from Zn23) and -2.63 e/Å³, respectively.

The refined composition is $\text{Sc}_{11.18(9)}\text{Mg}_{2.5(1)}\text{Zn}_{73.6(2)}$ or, normalized, $\text{Sc}_{12.8(1)}\text{Mg}_{2.9(1)}\text{Zn}_{84.3(2)}$, in comparison with the EDX result, $\text{Sc}_{14.2(2)}\text{Mg}_{2.8(2)}\text{Zn}_{83.0(2)}$. The slight difference in Sc/Zn ratios may correlate with uncertainties in the occupancies of atoms in the innermost tetrahedron (above). This structure represents the best ordered Tsai-type 2/1 ACs reported so far, with only three fractional positions. It should be noted that 2/1 ACs in general exhibit characteristically large numbers of relatively weak reflections (data), as reflected herein by the R_{int} value and the $R1$ value for all data (Table 1) and by the powder X-ray diffraction pattern as well (see ref 12).

Some data collection and refinement details for both crystals are summarized in Table 1. The atomic coordinates standardized with TIDY²³ are listed in Table 2 together with their isotropic equivalent displacement parameters. Anisotropic displacement parameters and selected bond distances are listed in Table S1 and Table S2 (Supporting Information).

Results and Discussion

Structure of 1/1 AC. This phase, $\text{Sc}_3\text{Mg}_{0.18(1)}\text{Zn}_{17.73(1)}$, crystallizes in the cubic space group $Im\bar{3}$ (No. 204), with $a = 13.863(2)$ Å. The lattice constant is very close to the expected value (13.87 Å) according to the experimental quasicrystal lattice constant.¹² It is a pseudo-binary derivative of ScZn_6 ²¹ and other isostructural MCD_6 ACs ($M = \text{Ca}$, rare-earth metal).⁷ It may also be described as the Mg terminus of the solution $\text{ScMg}_x\text{Zn}_{6-x}$, $x \leq \sim 0.06$, beyond which more Mg puts it close to the field of the 2/1 AC phase. As expected, there are no large differences between the present structure and those of the isostructural compounds.

The basic building block for the present structure is, as before,^{7,13,21} the complex triacontahedral cluster, within which the short-range-order (SRO) arrangement consists of four multiple-endohedral, interbonded polyhedral shells. These are, from the center out, a 3-fold disordered Zn_4 tetrahedron, a Zn_{20} pentagonal dodecahedron, a Sc_{12} icosahedron and a $(\text{Zn}, \text{Mg})_{30}$ icosidodecahedron. The composite of the inner four shells shown in Figure 1a defines the Tsai-type cluster.⁹ The atomic arrangement within the cluster is very similar to those described in detail previously,^{13,21} and we will not reiterate it. The outmost triacontahedral shell consists of 92 Zn atoms, 32 at the vertices and 60 at or near the midpoints of the edges (Figure 1b), all at radial distances of 7.10–8.16 Å. Of the 32 vertex positions, eight on the proper 3-fold axes are Zn5, and the others, Zn6. That is, all Zn1-Zn1-Zn1 triangular faces of the penultimate icosidodecahedral shell are capped by Zn5 atoms, whereas both the $\text{Zn1-Zn1-Zn1-Zn1-Zn7}$ pentagonal faces and the Zn1-

Table 2. Atomic Coordinates ($\times 10^4$) and Equivalent Isotropic Displacement Parameters (Å² $\times 10^3$) for $\text{Sc}_3\text{Mg}_{0.18(1)}\text{Zn}_{17.73(3)}$ and $\text{Sc}_{11.18(9)}\text{Mg}_{2.5(1)}\text{Zn}_{73.6(2)}$, the 1/1 and 2/1 AC, Respectively

		1/1 AC				
atoms	wyck.	occu. $\neq 1$	x	y	z	U_{eq}
Sc	24g		2010(1)	3097(1)	5000	8(1)
Zn1	48h		1173(1)	1995(1)	3409(1)	15(1)
Zn2	24g		0	3451(1)	4044(1)	10(1)
Zn3	24g		0	917(1)	2392(1)	28(1)
Zn4 ^b	24g	0.303(4)	0	797(5)	769(5)	108(3)
Zn5	16f		1621(1)	1621(1)	1621(1)	22(1)
Zn6	12c		0	1896(1)	5000	13(1)
Zn7/Mg	12d	0.878(9)/0.122	946(1)	5000	5000	25(1)

		2/1 AC				
atoms	wyck.	occu. $\neq 1$	x	y	z	U_{eq}
Sc1	24d		316(1)	4606(1)	1550(1)	6(1)
Sc2/Mg	24d	0.39/0.61(3)	345(2)	2329(2)	1558(2)	9(1)
Sc3	24d		1589(1)	4614(1)	3484(1)	6(1)
Sc4	24d		1603(1)	2314(1)	3462(1)	5(1)
Sc5	8c		408(1)	408(1)	408(1)	4(1)
Zn1	24d		93(1)	3467(1)	2175(1)	16(1)
Zn2	24d		308(1)	561(1)	4069(1)	13(1)
Zn3	24d		321(1)	542(1)	2749(1)	18(1)
Zn4	24d		326(1)	3433(1)	4711(1)	14(1)
Zn5	24d		361(1)	4400(1)	4075(1)	8(1)
Zn6	24d		369(1)	2518(1)	4069(1)	7(1)
Zn7	24d		385(1)	1563(1)	3465(1)	9(1)
Zn8	24d		479(1)	2619(1)	2856(1)	15(1)
Zn9	24d		519(1)	4280(1)	2853(1)	13(1)
Zn10	24d		608(1)	968(1)	1588(1)	10(1)
Zn11	24d		920(1)	3458(1)	3614(1)	12(1)
Zn12	24d		971(1)	1538(1)	4426(1)	8(1)
Zn13	24d		979(1)	1576(1)	2526(1)	9(1)
Zn14	24d		1008(1)	3467(1)	1470(1)	13(1)
Zn15	24d		1391(1)	4155(1)	4723(1)	17(1)
Zn16/Mg	24d	0.765(13)/0.235	1444(1)	2689(1)	4716(1)	18(1)
Zn17	24d		1460(1)	4349(1)	2153(1)	12(1)
Zn18	24d		1496(1)	2598(1)	2177(1)	17(1)
Zn19	24d		1769(1)	3475(1)	2830(1)	22(1)
Zn20	24d		2037(1)	3462(1)	3982(1)	22(1)
Zn21	24d		2482(1)	4428(1)	4447(1)	21(1)
Zn22	24d		2534(1)	4341(1)	2591(1)	28(1)
Zn23 ^b	24d	0.866(10)	3080(2)	3994(1)	3611(2)	62(2)
Zn24	24d		3474(1)	3993(1)	4887(1)	20(1)
Zn25	8c		1578(1)	1578(1)	1578(1)	9(1)
Zn26	8c	0.439(15)	2569(3)	2569(3)	2569(3)	27(4)
Zn27 ^b	8c	0.280(16)	2884(4)	2884(4)	2884(4)	22(5)
Zn28	8c		4466(1)	4466(1)	4466(1)	20(1)

^a U_{eq} is defined as one-third of the trace of the orthogonalized U_{ij} tensor. ^b Atoms forming the innermost tetrahedra. Other atoms with slightly larger isotropic thermal parameters are basically the neighboring atoms around the tetrahedron.

Zn1-Zn7 triangular faces are capped by Zn6. With $m\bar{3}$ symmetry, a triacontahedron has a total of ten 3-fold and fifteen 2-fold axes, proper or pseudo, plus, importantly, six pseudo 5-fold rotational axes. (A triacontahedron is the combination of an icosahedron and dodecahedron, with (a) vertices of the former over the faces, and on the (pseudo) 5-fold axes, of the latter, and (b) vertices of the dodecahedron on the 3-fold axes. The figure naturally exhibits a larger radial distance range because of the symmetry restrictions.) The triacontahedron has two sets of edge lengths: $d(\text{Zn5-Zn6}) = 5.042$ Å and $d(\text{Zn6-Zn6}) = 5.209$ Å. Interestingly, Zn2 atoms are almost linearly positioned at the centers of shorter edges, as indicated by $\angle \text{Zn6-Zn2-Zn6} = 179.7(1)^\circ$. On the contrary, Zn1 atoms occur somewhat off-center on the longer edges to give two different distances, Zn5-Zn1 (2.6082(9) Å) and Zn6-Zn1

(23) Gelato, L. M.; Parthé, E. *J. Appl. Crystallogr.* **1987**, *20*, 139.

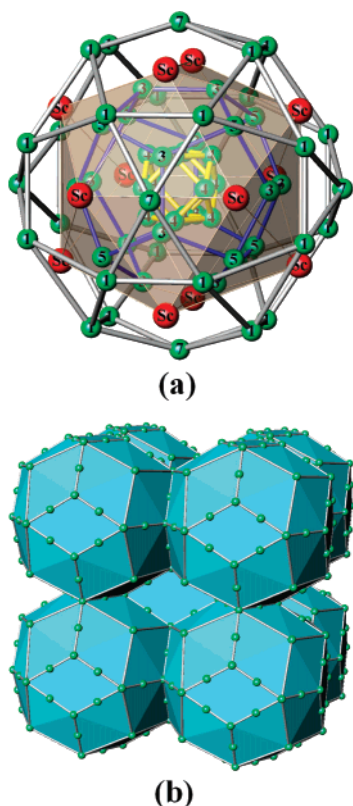


Figure 1. (a) Hierarchy of multiple endohedral shells within a triacontahedral cluster in the $\text{Sc}_3\text{Mg}_{0.18(1)}\text{Zn}_{17.73(3)}$ 1/1 AC, which are, from the center out, a 3-fold disordered tetrahedron (yellow bonds), a pentagonal dodecahedron (blue), an icosahedron (red atoms), and an icosidodecahedron (gray bonds). Numbers mark the atoms as listed in Table 2. All atoms in the innermost shell have 1/3 occupancies and are best described in terms of a tetrahedron disordered around the 3-fold axes, following Larson and Cromer.²² (b) Polyhedral view of b.c.c. arrangement of triacontahedral clusters in a unit cell of the 1/1 AC. Atoms near edge centers around the proper 3-fold axes are located beneath the surface and invisible. All Sc or Sc/Mg atoms are represented by arbitrary-sized red spheres, and the Zn or Zn/Mg atoms are represented by green, the same as in the following figures.

(2.7429(7) Å). In addition, small inward displacements of Zn1 also leave them invisible in this polyhedral view (Figure 1b). All of the Zn–Zn distances fall in the range of 2.511–2.938 Å and the Sc–Zn distances, 2.923–3.246 Å. For reference, both are in the neighborhood of, or greater than, Pauling’s single-bond metallic radii sums (CN: 12, Sc: 1.620, Zn: 1.339 Å²⁴).

The long-range-order (LRO) of the building blocks in the 1/1 AC is a body-centered-cubic (b.c.c.) packing of face-sharing or interpenetrating triacontahedra, as shown in Figure 1b. Following the global symmetry, the proper 3- and 2-fold axes of the triacontahedra lie along the body diagonals and edges of the unit cell, respectively. In this packing, each triacontahedron has 14 neighbors, six that share the Zn6–Zn6–Zn6–Zn6 rhombic faces along the 2-fold axes and eight that interpenetrate and share oblate rhombohedra (ORs) along the 3-fold axes, as highlighted in Figure 2. The vertex atoms in the 3-fold axes of the ORs are Zn5, which actually come from the dodecahedral shell in Figure 1a, whereas other six vertices are Zn6 atoms on the outermost triacontahedral shell. The Zn6–Zn6 and the Zn5–Zn6 edges of the ORs are, of course, also centered or nearly

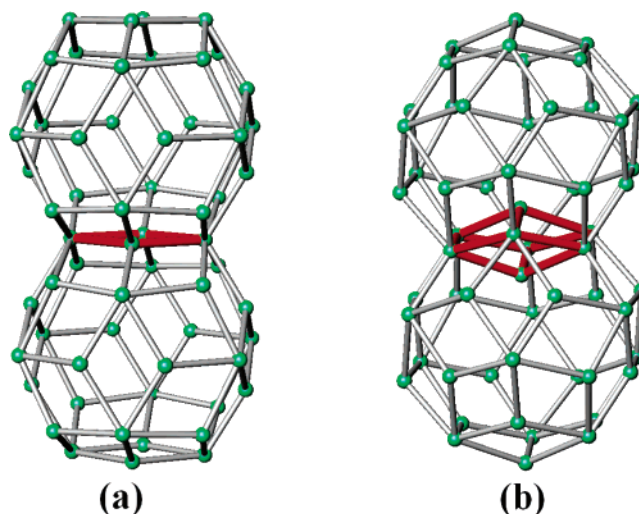


Figure 2. The connections between neighboring triacontahedral clusters in the 1/1 AC along (a) the 2-fold axes and (b) the 3-fold axes. For clarity, the triacontahedra are shown with vertex atoms only. Although the triacontahedra in the 2/1 AC have different atom identities and symmetries, they have the same linkages (see text).

centered by Zn2 and Zn1, respectively (see Figure S2, Supporting Information).

Structure of 2/1 AC. $\text{Sc}_{11.18(9)}\text{Mg}_{2.5(1)}\text{Zn}_{73.6(2)}$ crystallizes in the cubic space group $Pa\bar{3}$ (No. 205), with $a = 22.412$ (2) Å. The cell parameter of the 2/1 AC is close to τ times that of the 1/1 AC, typical for two ACs in the consecutive order of the Fibonacci series.⁴

The 2/1 AC also consists of triacontahedral clusters as the fundamental building blocks plus prolate (acute) rhombohedral (PR) clusters that are condensed with the former by sharing rhombic faces. The primitive cubic packing of both types of clusters in the unit cell is shown in Figure 3a. The centers of the triacontahedra are located at the special $8c$ (0.346, 0.346, 0.346) and equivalent positions. The triacontahedral clusters are very similar to those in the 1/1 AC, but of course, they exhibit more flexibility in both positions and distances because of the reduced symmetry (.3. rather than $m\bar{3}$). (According to the deposited crystallographic data, the centers of triacontahedral clusters in the $\text{Ca}_{13}\text{Cd}_{76}$ ¹⁷ also lie very close to these positions.) The centers of the PRs are, in comparison, located at the cell origins and face centers (Wyckoff $4a$ positions, $\bar{3}$. symmetry); therefore, there are in all four ($= 1/8 \times 8 + 1/2 \times 6$) PRs in the unit cell.

Figure 3b shows the SRO of the inner four shells within the triacontahedron (an expanded view is also available as Figure S3, Supporting Information). As can be seen, the innermost shell is now a defect tetrahedron rather than the 3-fold disordered tetrahedron in the 1/1 AC. This unit is generated by a fractional $8c$ Zn27 and three $24d$ Zn23 atoms, with $d(\text{Zn27} - \text{Zn23}) = 2.98$ (1) Å and the basal $d(\text{Zn23} - \text{Zn23}) = 2.516$ (5) Å. The tetrahedral shell is not ideally concentric with the outer shells (as in the 1/1 AC); rather, it is displaced outward in the direction of Zn27 along the proper 3-fold axis. The displacement results in a short formal distance (~ 1.24 Å) between Zn27 and another fractional atom, Zn26 in the next dodecahedron shell. However, these three sites are all fractionally occupied, the only such positions in the 2/1 AC, and they naturally exhibit somewhat larger standard deviations and displacement parameters (Table 2). Beyond the tetrahedral shell, there are successively a $\text{Zn}_{19,4}$

(24) Pauling, L. *The nature of the chemical bond*, 3rd ed.; Cornell University Press: Ithaca, 1960; p 393–448.

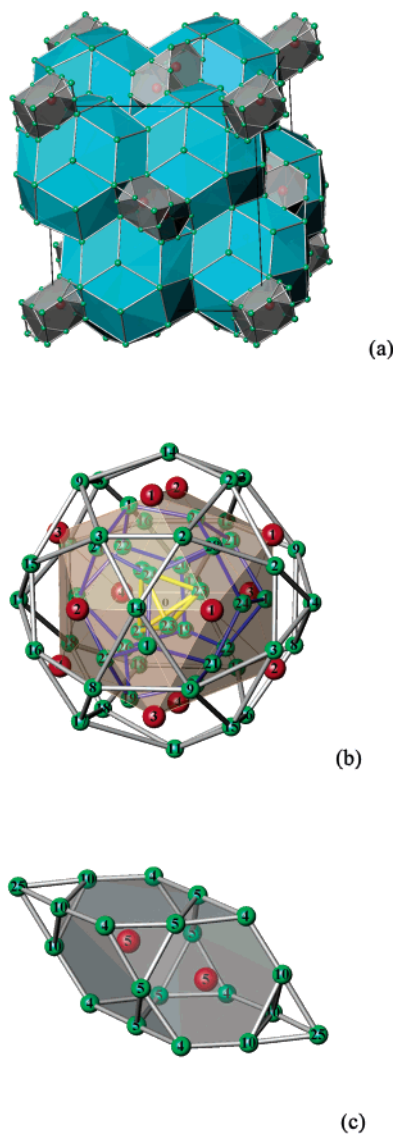


Figure 3. (a) Polyhedral view of the primitive cubic unit cell in the $\text{Sc}_{1.118(9)}\text{Mg}_{2.5(1)}\text{Zn}_{73.6(2)}$ 2/1 AC in terms of triacontahedra (blue) and the intervening prolate rhombohedra (gray). For clarity, atoms at or near the midpoints of all edges on the former are not shown. (b) Hierarchy of multiply endohedral shells within each triacontahedral cluster. The shells are, from the center out, a defect tetrahedron (yellow bonds), a pentagonal dodecahedron (blue), an icosahedron (red atoms), and an icosidodecahedron (gray). Numbers mark the atoms as listed in Table 2. All Sc or Sc/Mg atoms are marked by red spheres, and the Zn or Zn/Mg atoms are marked by green spheres. Expanded views of these shells are given in figure S3, together with a triacontahedral shell. (c) The construction of a PR in the 2/1 AC. The double Friauf polyhedron shown in gray is centered by a Sc–Sc dimer (red).

dodecahedral shell with radial distances of 3.40–4.05 Å, a $\text{Sc}_{10.2}\text{Mg}_{1.8}$ icosahedral shell at 4.89–4.93 Å, and a $\text{Zn}_{29.3}\text{Mg}_{0.7}$ icosidodecahedral shell at 5.60–5.78 Å. The composite of these four shells defines a modified Tsai-type cluster. This is again encapsulated within a triacontahedral shell of 92 Zn atoms with radial distances of 6.98–8.25 Å. The Sc–Zn distances in the 2/1 AC exhibit a wider range, 2.858–3.324 Å, about 0.1 Å more or less than in the 1/1 AC. A similar situation occurs for the Zn–Zn distances, within 2.473–3.192 Å. However, these flexibilities have negligible influences on the size of the different shells, that is, the outmost triacontahedron retains the same average edge length (5.11 Å) as that in the 1/1 AC.

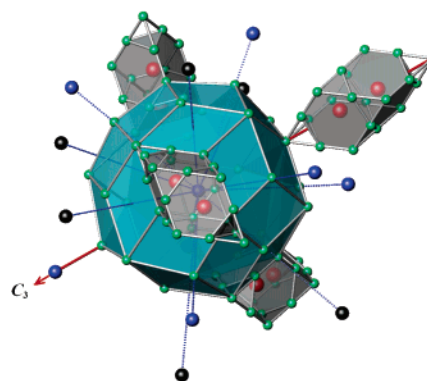


Figure 4. Environment of a triacontahedral cluster in 2/1 AC, showing the linkages among triacontahedra and prolate rhombohedra (gray). For clarity, only the central triacontahedron (A) is shown; the other 13 like neighbors are represented by spheres at their centers. Of the 13, the six black ones lie on center-to-center dashed lines that pass through the centers of rhombic faces shared with A, and other seven blue, on lines that pass through proper or pseudo 3-fold vertices and share ORs with A (Figure 2). All atoms inside of or on or near the midpoints of the edges of triacontahedra on A are omitted. The proper 3-fold axis is marked.

Figure 3c shows the SRO of the PR, in which a Sc–Sc dimer [$d(\text{Sc5}–\text{Sc5}) = 3.166 \text{ \AA}$] is centered on the long 3-fold diagonal. These Sc atoms are also at the centers of a double Friauf polyhedra (gray polyhedra in Figures 3a and 3c) after the two Zn25 atoms on the long diagonal (shared with neighboring triacontahedra) are excluded. In $\text{Ca}_{13}\text{Cd}_{76}$,¹⁷ only triacontahedra and double Friauf polyhedra (with dimers) were noted, but not PRs. (A double Friauf polyhedron is a truncated PR.) Each PR is bounded by eight triacontahedral clusters: two that share the Zn25 vertices with the PR, and six that share the Zn 4–Zn4–Zn4–Zn25 rhombic faces. Therefore, the PRs can be alternatively viewed as cavities that are automatically generated by primitive cubic packing of the fundamental triacontahedral clusters via shared atoms on the rhombic faces, Figure 3a. In this case, the dimers can be called “glue atoms”, those that do not belong to the basic building blocks in the jargon of QCs.¹

Figure 4 shows the environment of a triacontahedron in the 2/1 AC, which also illustrates the linkages between a triacontahedral cluster and the PRs. For clarity, only the central triacontahedral cluster (A) is shown as a polyhedron, whereas like neighbors are denoted by the solid spheres marking their centers. As can be seen, each triacontahedron has 13 like and 4 PR neighbors arranged with C_3 symmetry. Of the 13 neighbors, six (black) lie on the center-to-center dotted lines that pass through rhombic faces of A that are shared between the two. The other seven (blue) lie on 3-fold axes, pseudo or proper, and share ORs with A (Figure 2b). These are very similar to the linkages in the 1/1 AC except that the latter all involve proper 3-fold axes.

Triacontahedral clusters are not unique to the present study as they exist in other Tsai-type ACs.^{7,13,17} They are also found in the Bergman-type ACs Al_5CuLi_3 (1/1)²⁵ and Al–Mg–Zn (2/1)²⁶ and in the i-QC models described earlier by Audier and Guyot.^{1,27,28} These regularities shed new light on condensation models for both ACs and i-QCs. For example, adoption of stuffed triacontahedral clusters as the fundamental building blocks for the 1/1 ACs, rather than the smaller Tsai-type clusters

(25) Audier, M.; Pannetier, J.; Leblanc, M.; Janot, C.; Lang, J.-M.; Dubost, B. *Physica B (Amsterdam)* **1988**, *153*, 136.

(26) Lin, Q.; Corbett, J. D. *Proc. Nat. Acad. Sci.* **2006**, *103*, 13589.

within them, has the advantage that all of the “glue” (dimer) atoms, which are usually under-emphasized in the literature, are naturally included.

In particular, the identification of PRs (along with triacontahedra) in ACs offers very useful information for structural modeling of i-QC. Takakura and co-workers²⁹ have recently noted a Yb–Cd i-QC model based on triacontahedra and acute rhombohedra according to a further consideration of the reported structure of the Yb₁₃Cd₇₆ 2/1 ACs.¹⁷ In this case, the appearances of both PRs and ORs in the 2/1 AC remind us that the structure can alternatively be described with atom-decorated 3D Penrose tiles (PR and OR)³⁰ inasmuch as a triacontahedron can also be decomposed into 10 ORs and 10 PRs. Thus, a Penrose tiling model for the corresponding Sc–Mg–Zn i-QC would require only small shifts of the atoms in the 2/1 AC. Actually, we have found a more straightforward route to construct a real-space i-QC model from the structural data of the two present ACs.¹⁵ However, this is beyond the purpose of the present article.

- (27) Audier, M.; Guyot, P. In *Quasicrystalline Materials*; Janot, C., Dubois, J. M., Eds.; World Scientific: Singapore, 1988; pp 181–194.
- (28) Audier, M.; Guyot, P. In *Extended Icosahedral Structures*; Jarić, M. V., Gratiás, D., Eds.; Academic Press Inc.: Harcourt Brace Jovanovich, 1989; pp 1–36.
- (29) Takakura, H.; Pay Gómez, C.; Yamamoto, A.; Boissieu, M. D.; Tsai, A. P. In *Abstracts, 9th Int. Conf. on Quasicrystals*; Iowa State University: Ames, IA, 2005.
- (30) Penrose, B. *Bull. Inst. Math. Appl.* **1974**, *10*, 266.

Conclusions

In summary, the following two main points are evident from the detailed structural analyses of Sc₃Mg_{0.18(1)}Zn_{17.73(3)} and Sc_{11.18(9)}Mg_{2.5(1)}Zn_{73.6(2)}, the respective 1/1 and 2/1 ACs of the Sc–Mg–Zn i-QC:

(1) Building blocks for both ACs at the unit cell level are consistently triacontahedral clusters, rather than the so-called Tsai-type clusters within them. Both ACs have similar SRO structural motifs and very similar linkages among the triacontahedral clusters.

(2) The differences between the two ACs lie mainly in the LRO of the triacontahedral clusters. In contrast to the b.c.c. packing in the 1/1 AC, the less condensed primitive cubic packing in the 2/1 AC automatically generates PR cavities, and these are centered by Sc–Sc dimers.

Acknowledgment. This work has been supported by the U.S. National Science Foundation, Solid-State Chemistry, via grants DMR-0129785 and -0444657, and has been performed in facilities of the Ames Laboratory, U.S. Department of Energy.

Supporting Information Available: Figures S1–S3, Tables S1–S2, and two CIF files. This material is available free of charge via the Internet at <http://pubs.acs.org>.

JA063897U